

Research Article

Synthesis of Ag-Au Nanoparticles by Galvanic Replacement and Their Morphological Studies by HRTEM and Computational Modeling

Manuel Ramos,^{1,2} Domingo A. Ferrer,³ Russell R. Chianelli,¹ Victor Correa,⁴ Joseph Serrano-Matos,⁴ and Sergio Flores²

¹ Materials Research and Technology Institute, UT-El Paso, 500W Univesity Ave., Burges Hall Rm. 303, El Paso, TX 79902, USA

² Departamento de Física y Matemáticas, Universidad Autónoma de Ciudad Juárez, Cd. Juárez, Chihuahua C.P. 32300, Mexico

³ Microelectronics Research Center, University of Texas at Austin, Austin, TX 78758, USA

⁴ Departamento de Ciencias y Tecnología, Universidad Metropolitana, San Juan, PR 00928, Puerto Rico

Correspondence should be addressed to Manuel Ramos, maramos1@miners.utep.edu

Received 13 October 2010; Revised 22 November 2010; Accepted 27 December 2010

Academic Editor: Shaogang Hao

Copyright © 2011 Manuel Ramos et al. This is an open access article distributed under the Creative Commons Attribution License, which permits unrestricted use, distribution, and reproduction in any medium, provided the original work is properly cited.

Bimetallic nanoparticles are important because they possess catalytic and electronic properties with potential applications in medicine, electronics, and chemical industries. A galvanic replacement reaction synthesis has been used in this research to form bimetallic nanoparticles. The complete description of the synthesis consists of using the chemical reduction of metallic silver nitrite (AgNO_3) and gold-III chloride hydrate (HAuCl) salt precursors. The nanoparticles display round shapes, as revealed by high-resolution transmission electron microscope (HRTEM). In order to better understand the colloidal structure, it was necessary to employ computational models which involved the simulations of HRTEM images.

1. Introduction

Synthesis and characterization of nanocrystals have been a research topic of high interest in recent decades due to their potential application in medical (cancer imaging), optical physics, catalysis, engineered materials, and electronics [1–6]. Achievement of specific particle morphology depends solely on right combination of precursors, as well as suitable selection of temperature and capping agents [7].

Presently, one can find several articles where full explanations are included in chemical synthesis techniques to attain specific particle morphologies, along with their potential applications [8]. Monometallic nanoparticles are assumed to have three basic shapes: decahedral, cubo-octahedral, and icosahedral. Nanoparticles geometry and facets are made out of (111) planes as observed in icosahedron; and is attributed to lowest surface energy $\gamma_{(111)}$ of nucleation in (111)-plane; this implies a large internal core-strain values. Cubo-octahedron presents no internal core-strain and significant large surface energy constituted primarily by (111) and (100)

facets, whereas decahedron has moderate internal strain and smaller facets made of (111) and (100) planes. The following is concluded regarding monometallic nanoparticles: $\gamma_{(111)} < \gamma_{(100)} < \gamma_{(110)}$ as indicated by Lee and Meisel [9].

Previous theoretical work indicates that the addition of a second metal, when synthesizing nanoparticles, can lead to a significant change on its physical-chemical properties, as reflected also on particle morphology (i.e., core-shell, spherical, and truncated-icosahedral). Very little is known about bimetallic nanoparticles in terms of its crystallographic structure, shape, and location of bimetallic precursors, which can attract attention when studying bimetallic systems.

In order to understand the difference between bimetallic nanoalloy and bulk systems, Yonezawa and Toshima proposed that some bimetallic nanoalloys (i.e., Au-Ag, Au-Pd) seem to exist due to miscibility gaps at certain compositions ratio (i.e., 20%, 30%, and 10%) provoking the formation of a nanoalloy [10]. Nanoalloy formation could be attributed to the differences in atomic radii and electron migration allowing atoms to accommodate, showing shell periodicity

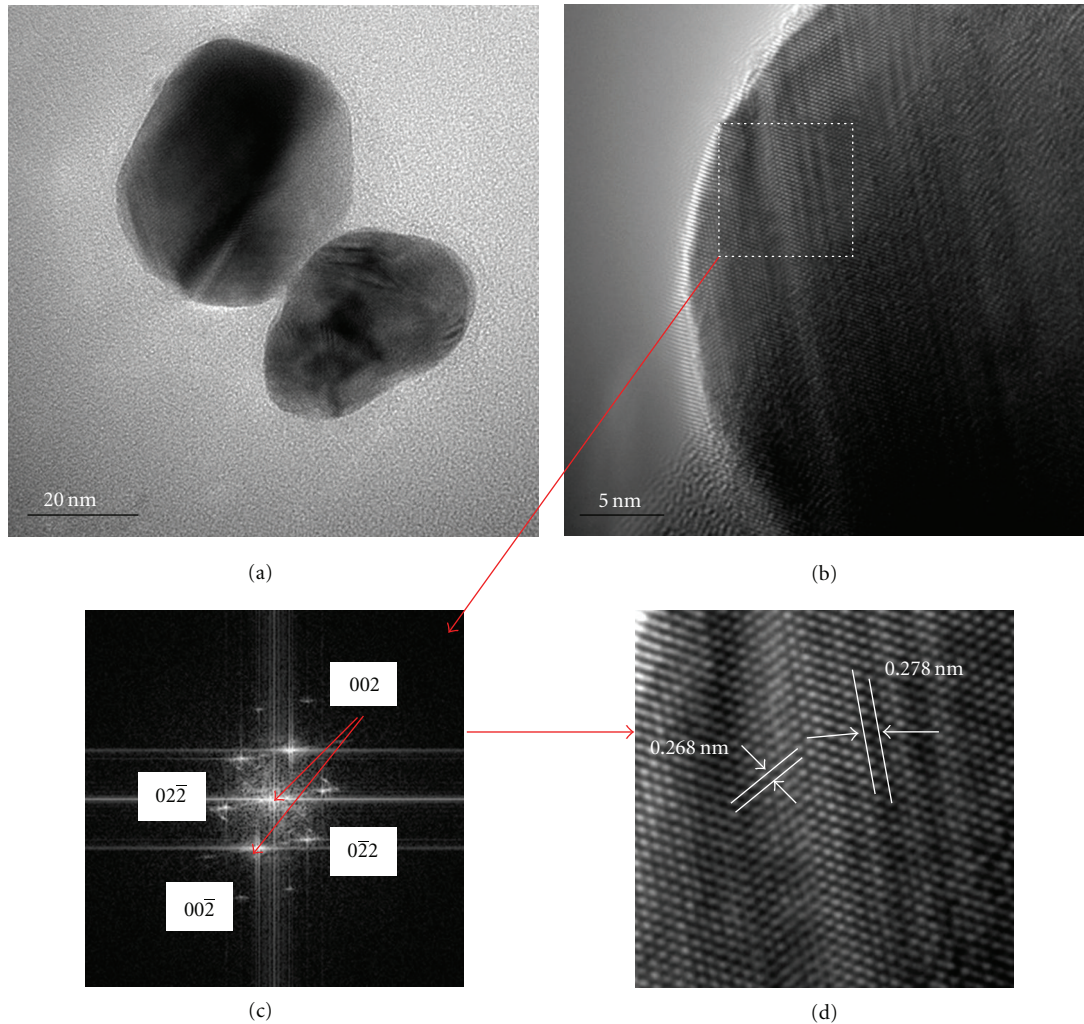


FIGURE 1: (a) 20 nm resolution HRTEM image of spherical shape Ag-Au nanoparticles. (b) 5 nm resolution HRTEM image showing lattice distances. (c) Select area diffraction with $(00\bar{2})$, $(0\bar{2}2)$, and $(0\bar{2}2)$ principal reflections. (d) Inverse Fast Fourier Transform of SAD presented in (c).

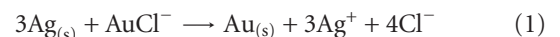
(i.e., onion array layers) as observed by conventional electron microscopy techniques [11].

We present a successful chemical synthesis from Au and Ag salt precursors for bimetallic spherical nanoparticles. Bimetallic particle formation is attributed to a galvanic replacement reaction and shape. Bimetallic composition was confirmed by high resolution transmission electron microscope (HRTEM) results, as well as computational simulations for reconstruction of HRTEM images.

2. Experimental

Two precursor solutions were used for chemical synthesis of bimetallic Ag-Au nanoparticles. The first solution was made dissolving 90 mg of silver nitrite (AgNO_3) in 500 mL of distilled water; later a mixture was added. It was made with 1% sodium citrate dissolved in 10 mL of distilled water, which was brought and kept for 1 h to boiling temperature

100°C. Then a separate second solution that consisted of 240 mg of gold-III chloride hydrate (HAuCl_4) dissolved in 500 mL of deionized water at 100°C with the addition of a mixture of 1% sodium citrate and 50 mL of distilled water. Finally, both precursor solutions were mixed together and subjected to vigorous stirring at constant temperature of 100°C for 1 h. The stoichiometric equation for particle formation of Ag-Au galvanic reaction is presented as follows:



and seems to be in agreement with [12].

3. Results and Discussion

Particle size, shape, and morphology were studied by HRTEM on an FEI Tecnai TF20 equipped with an STEM unit, high-angle annular dark-field (HAADF) detector, and X-Twin lenses. Sample preparation was done by dissolving

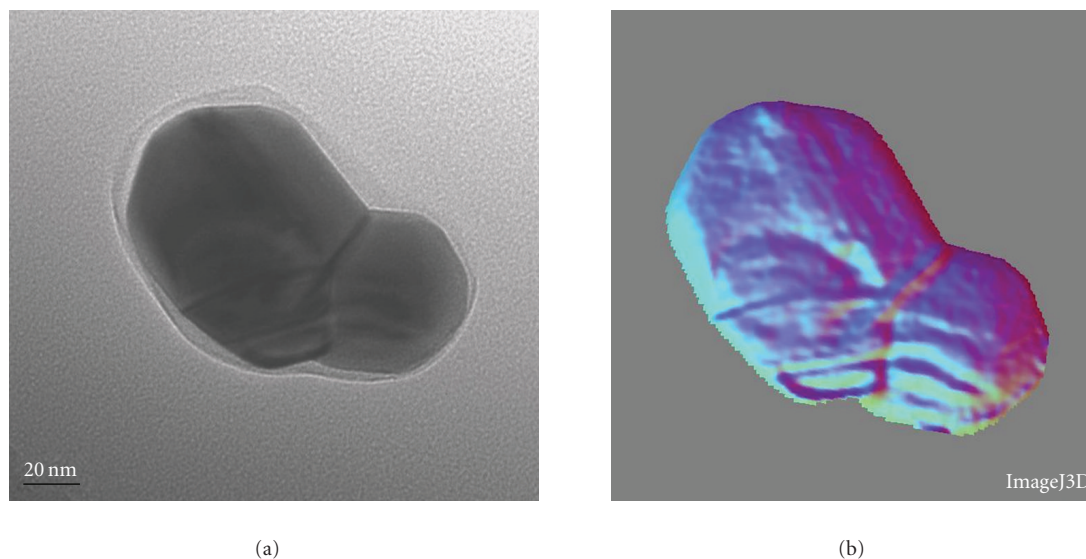


FIGURE 2: (a) HRTEM of elbow-like nanoparticle, formed by accommodation of three small Ag-Au nanoparticles. (b) 3D reconstruction image of (a) performed by ImageJ package.

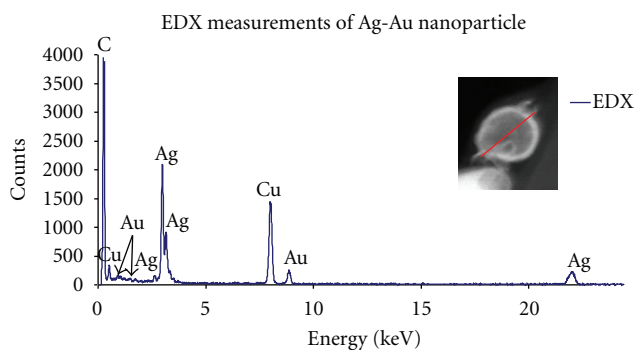


FIGURE 3: EDX results of Ag-Au nanoparticles, Cu and C signals are from TEM grid, inset dark field scanning transmission electron image.

0.5 milligrams in isopropanol placed in an ultrasonic bath for dispersion of nanoparticle clusters. One drop of the solution was used for HRTEM on lacey/carbon (EMS LC225-Cu) grids. Operational voltage was 200 kV in both dark field (DF) and bright field (BF) mode images, with Scherzer defocus condition at $\Delta f_{\text{Sch}} = -1.2(C_s\lambda)^{1/2}$. Energy-dispersive X-ray analysis, EDX was performed while TEM using a solid angle of 0.13 sr detector.

Atomic percentage of gold found was about 13% from EDX results, which was confirmed from calculated molar concentration on both precursor solutions; ratios of AuCl_4 ions with respect to silver were roughly 10%, indicating that for each gold atom there are three silver neighbors present. The percentages were consistent, since lattice parameters in both metals are very similar, for Au-lattice ~ 0.4078 nm and Ag-lattice ~ 0.4086 nm for typical FCC bulk structures. Figure 1(a) presents two round spherical shapes Ag-Au

nanoparticles, Figure 1(b) corresponds to a section of Figure 1(a) at 5 nm of resolution, Figure 1(d) is presenting atomistic distances for [111] and [121] planar directions with atomistic distances of 0.268 nm and 0.278 nm for Au and Ag atoms, respectively; select area of diffraction indicate $(02\bar{2})$, $(0\bar{2}2)$, and $(00\bar{2})$ as principal planar reflections.

Grain boundary was observed for spherical truncated nanoparticles as presented in Figure 2(a). Grain boundary can be understood in terms of surface energy thermodynamics and attributed also to the ionic interaction between specimens as proposed by Elechiguerra et al. for nanorods formation [13]. A 3D reconstruction image is presented in Figure 2(b); the image was reconstructed using ImageJ package. Figure 3 presents EDX results; the two major peak signals correspond to C/Cu content on TEM diffraction grids; gold shows energy intensities at 2 keV and 2.6 keV, whereas for silver, intensities are observed at 3 keV and 3.4 keV. Using A ccelrys Materials Studio, a computational nanoparticle model was done. The model was subjected to TEM simulations using a full dynamical calculation by multislice method [14]. The TEM simulator is based on projected potential $f(U) = \sum_{i=1}^n a_i e^{-ibU^2}$, where U represents coordinates in reciprocal space (u, v, w) . Results from TEM simulations are presented in Figure 4 and seem to be consistent with experimental HRTEM presented on Figure 2(a).

4. Conclusion

A successful synthesis to produce nanoparticles gold and silver precursor solutions is presented here. Bimetallic Ag-Au nanoparticles were formed due to a galvanic replacement reaction, which consists of the migration of ionic Ag and Au atoms from salt precursors at boiling temperature. Products

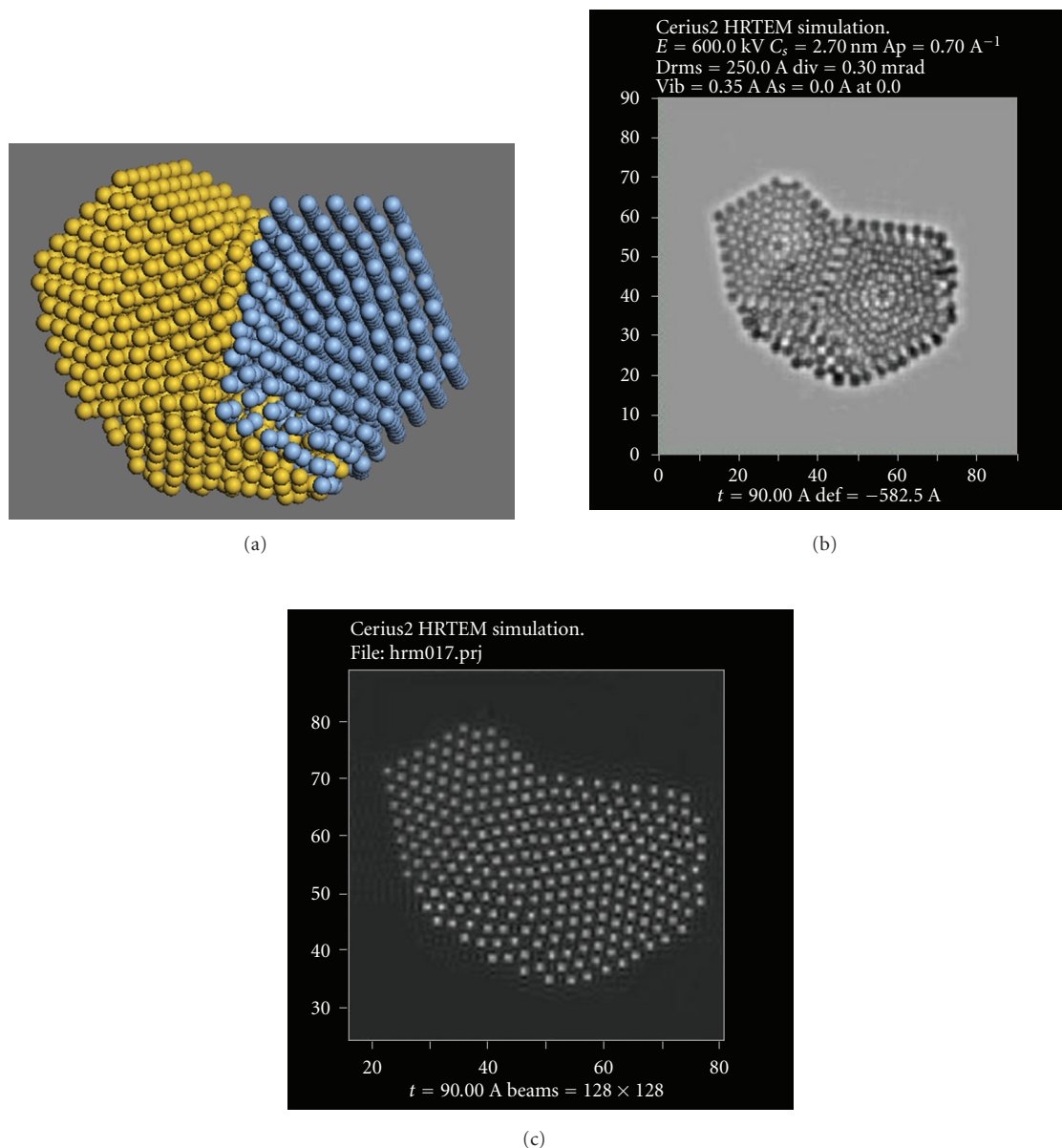


FIGURE 4: (a) Computer assisted Ag-Au nanoparticle (Ag-blue and Au-yellow) used to understand HRTEM image presented in 2. (b) TEM simulation of (a) (Ag-Au nanoparticles) for comparison with experimental HRTEM images.

were analyzed by HRTEM and EDX techniques. EDX results show energy intensity peaks at 2 keV and 2.6 keV for gold and 3 keV and 3.4 keV for silver. Particle shape was studied by computational modeling for specific elbow-like shape for three small Ag-Au nanoparticles. The model was subjected to TEM simulations using full dynamical projected potential. The authors will start testing synthesized Ag-Au nanoparticles as contrasting agents in cancer mapping for biotissue during magnetic resonance imaging (MRI) studies [15].

Acknowledgments

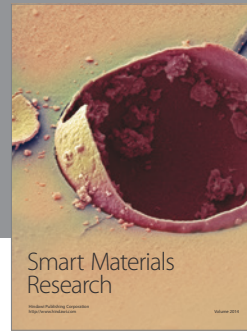
The authors thank the Consejo Nacional de Ciencia y Tecnología, México for their economic support, the National

Nanotechnology Infrastructure Network (NNIN) Research Program of the Microelectronic Research Center of UT-Austin, and the Materials Research and Technology Institute of UT-El Paso for usage of research facilities.

References

- [1] N. Toshima and T. Yonezawa, "Preparation of polymer-protected gold/platinum bimetallic clusters and their application to visible light-induced hydrogen evolution," *Makromolekulare Chemie, Macromolecular Symposia*, vol. 59, pp. 281–295, 1992.
- [2] D. Garcia-Gutierrez, C. Gutierrez-Wing, M. Miki-Yoshida, and M. Jose-Yacaman, "HAADF study of Au-Pt core-shell

- bimetallic nanoparticles,” *Applied Physics A*, vol. 79, no. 3, pp. 481–487, 2004.
- [3] J. Chen, B. Wiley, Z. Y. Li et al., “Gold nanocages: engineering their structure for biomedical applications,” *Advanced Materials*, vol. 17, no. 18, pp. 2255–2261, 2005.
- [4] G. A. Hussein and W. G. Pitt, “Micelles and nanoparticles for ultrasonic drug and gene delivery,” *Advanced Drug Delivery Reviews*, vol. 60, no. 10, pp. 1137–1152, 2008.
- [5] T. Paulmier, J. M. Bell, and P. M. Fredericks, “Plasma electrolytic deposition of titanium dioxide nanorods and nano-particles,” *Journal of Materials Processing Technology*, vol. 208, no. 1-3, pp. 117–123, 2008.
- [6] V. Vashchenko, A. Krivoshey, I. Knyazeva, A. Petrenko, and J. W. Goodby, “Palladium-catalyzed Suzuki cross-coupling reactions in a microemulsion,” *Tetrahedron Letters*, vol. 49, no. 9, pp. 1445–1449, 2008.
- [7] L. Rivas, S. Sanchez-Cortes, J. V. García-Ramos, and G. Morcillo, “Mixed silver/gold colloids: a study of their formation, morphology, and surface-enhanced Raman activity,” *Langmuir*, vol. 16, no. 25, pp. 9722–9728, 2000.
- [8] N. N. Kariuki, J. Luo, M. M. Maye et al., “Composition-controlled synthesis of bimetallic gold-silver nanoparticles,” *Langmuir*, vol. 20, no. 25, pp. 11240–11246, 2004.
- [9] P. C. Lee and D. Meisel, “Adsorption and surface-enhanced Raman of dyes on silver and gold sols,” *Journal of Physical Chemistry*, vol. 86, no. 17, pp. 3391–3395, 1982.
- [10] T. Yonezawa and N. Toshima, “Polymer- and micelle-protected gold/platinum bimetallic systems. Preparation, application to catalysis for visible-light-induced hydrogen evolution, and analysis of formation process with optical methods,” *Journal of Molecular Catalysis*, vol. 83, no. 1-2, pp. 167–181, 1993.
- [11] J. M. Montejano-Carrizales, J. L. Rodriguez-Lopez, C. Gutierrez-Wing, M. Miki-Yoshida, and M. Jose-Yacaman, “Crystallography and shape of nanoparticles and clusters: geometrical analysis, image, diffraction simulation and high resolution images,” in *Encyclopedia of Nanoscience and Nanotechnology*, H. S. Nalwa, Ed., vol. 2, pp. 237–282, American Scientific Publishers, Los Angeles, Calif, USA, 2004.
- [12] J. Chen, B. Wiley, Z. Y. Li et al., “Gold nanocages: engineering their structure for biomedical applications,” *Advanced Materials*, vol. 17, no. 18, pp. 2255–2261, 2005.
- [13] J. L. Elechiguerra, J. Reyes-Gasga, and M. J. Yacamán, “The role of twinning in shape evolution of anisotropic noble metal nanostructures,” *Journal of Materials Chemistry*, vol. 16, no. 40, pp. 3906–3919, 2006.
- [14] A. Gómez-Rodríguez, L. M. Beltrán-del-Río, and R. Herrera-Becerra, “SimulaTEM: multislice simulations for general objects,” *Ultramicroscopy*, vol. 110, no. 2, pp. 95–104, 2010.
- [15] P. K. Jain, I. H. ElSayed, and M. A. El-Sayed, “Au nanoparticles target cancer,” *Nano Today*, vol. 2, no. 1, pp. 18–29, 2007.



Hindawi

Submit your manuscripts at
<http://www.hindawi.com>

